Journal of Chemical Health Risks

www.jchr.org

JCHR (2025) 15(5), 306-319 | ISSN:2251-6727

Spatially Informed Public Health Responses to COVID-19 in Asia: Evidence from Advanced Spatial Regression Techniques

Megha Sharma*, Shalini Chandra

Department of Mathematics and Statistics, Banasthali Vidyapith, Rajasthan, India

(Received: 16 July 2025 Revised: 20 August 2025 Accepted: 02 September 2025)

KEYWORDS

COVID-19; Spatial Analysis; Robust Geographically Weighted Regression; Public Health Modeling; Outliers and Heteroscedasticity; Regional Health Disparities.

ABSTRACT:

Understanding the spatial dynamics of COVID-19 is essential for designing effective and equitable public health responses. However, most existing analyses have relied on traditional regression or basic spatial models, often failing to capture the complex, multi-dimensional nature of infectious disease spread. This study highlights the importance of adopting flexible, data-driven approaches that account for both statistical and spatial heterogeneity in pandemic data. Using data from Asian countries, we examined geographic variation in COVID-19 cases and deaths through a combination of classical, robust, and spatial regression models. Preliminary analysis revealed non- normal distributions, extreme outliers, and significant spatial clustering—underscoring the need for robust, spatially aware modeling. Robust Weighted Least Squares (RWLS) was first applied to handle heteroscedasticity and outliers. The detection of spatial dependence prompted the use of spatial models including the Spatial Lag Model (SLM), Spatial Error Model (SEM), and Geographically Weighted Regression (GWR). While GWR addressed spatial non-stationarity, it remained sensitive to outliers. To overcome this, we employed a Robust Geographically Weighted Regression (RGWR) model that integrates Huber loss and optimal bandwidth selection. RGWR outperformed all other models, explaining 91% and 92% of the variance in case and death rates, respectively, and revealed substantial regional heterogeneity in predictor influence. Key drivers of COVID-19 outcomes included the proportion of elderly population, air pollution levels, and healthcare infrastructure. By integrating distributional, spatial, and robustness dimensions of the data, this study demonstrates that nuanced, context-sensitive analysis can yield more reliable and actionable insights, supporting better-targeted public health interventions and resource allocation.

1. Introduction

Although the immediate threat of COVID-19 has subsided, its widespread impact continues to provide valuable insights for ongoing research. Investigating the factors that influenced its transmission and severity remains essential—particularly in Asian countries, which experienced major economic setbacks, rising unemployment, and significant strain on healthcare infrastructure (Sardar et al. (2020); Chaurasia et al. (2021); Kumar and Awasthi (2020); Chandra and Sharma (2024)). The pandemic exposed underlying social inequalities that heightened vulnerability to infection (Ahmed et al. (2020)), including overcrowded living conditions (Pereira and Oliveira (2020)), high population density (Rocklöv and Sjödin (2020)), and limited access to healthcare, and large populations of at-risk individuals (Dutta et al. (2021)). Environmental conditions such as temperature, were also linked to variations in disease severity across different countries (Chen et al. (2020); Tosepu et al. (2020); Chung et al. (2021); Bashir et al. (2020)). Moreover, factors like urban slum settlements (Sridhar (2023)), smoking behavior, and other socio-behavioral

Journal of Chemical Health Risks
www.jchr.org
JCHR (2025) 15(5), 306-319 | ISSN:2251-6727

determinants contributed to inequalities in exposure risk and access to healthcare services.

Various methodological approaches have been employed to analyze the dynamics of COVID-19, with foundational models playing a critical role in early-stage research. These include classical regression methods such as Ordinary Least Squares (OLS), alongside key spatial modeling techniques like Spatial Lag Model (SLM), Spatial Error Model (SEM), and Geographically Weighted Regression (GWR) (Chi et al. (2021); Desjardins et al. (2020); Sarkar et al. (2021); Ramírez-Aldana et al. (2020); Appiah-Otoo and Kursah (2022); Adekunle et al. (2020)). While these models provided valuable insights, they are based on several statistical assumptions—namely, the absence of multicollinearity, homoscedasticity, normally distributed residuals, and minimal influence of outliers. In practice, such assumptions are frequently violated in real-world public health data, especially in the context of the COVID-19 pandemic, which is characterized by high variability, structural heterogeneity, and non-standard data distributions. These challenges highlight the need for more robust and adaptable modeling frameworks capable of addressing the complexities inherent in pandemic data (Sharma and Chandra (2024)).

To handle data irregularities, this study incorporates several of these frameworks, including Robust Weighted Least Squares (RWLS) for addressing heteroscedasticity and outliers, as well as spatial econometric models such as SLM and SEM to account for spatial dependence (Anselin (1988); Elhorst (2014)). Additionally, GWR is employed to capture spatial non-stationarity in model parameters (Fotheringham et al. (2002)). These methods provide a comprehensive basis for understanding the geographic variability in COVID-19 outcomes. Despite its usefulness, GWR is sensitive to data irregularities such as outliers, heteroscedasticity, and multicollinearity—common features in large-scale epidemiological datasets. These issues can compromise the reliability of local estimates, underscoring the need for more robust modeling strategies. Recent advancements in spatial modeling have introduced robust extensions of GWR, which reduce the influence of extreme values and accommodate variability in data quality across regions (Fotheringham et al. (2002); LeSage (2004)).

Among recent advancements, the Robust Geographically Weighted Regression (RGWR) framework integrated with Huber loss has demonstrated significant potential for handling spatial heterogeneity and outlier influence in pandemic-related data (Zhang and Mei (2011); Chen et al. (2012)). This model enhances estimation robustness by combining Huber's M-estimation, which mitigates the impact of extreme residuals, with spatial weighting to capture local variations in relationships across regions. By replacing the traditional least squares criterion with the Huber loss function, RGWR provides a balance between efficiency for normally distributed errors and resistance to outliers.

Moreover, the RGWR framework also supports data-driven bandwidth selection, which optimizes the spatial kernel's smoothness, thereby improving both local fit and predictive accuracy. This makes it especially suitable for complex epidemiological datasets such as those arising from COVID-19. This study applies RGWR approach to COVID-19 data from Asian countries, aiming to identify region-specific risk factors and uncover spatial disparities in transmission patterns. In doing so, a comprehensive suite of predictive models was employed, including classical regression (e.g., ordinary least squares) and spatial models (e.g., SLM, SEM, and GWR) along with their robust extensions to evaluate how predictive modeling can enhance the accuracy and interpretability of COVID-19 outcomes. The performance of these models was compared using metrics such as Adjusted R^2, Root Mean Square Error (RMSE), and information criteria (AIC/BIC). By focusing on Asia—a region characterized by sharp contrasts in demographic, environmental, and socioeconomic conditions—this analysis contributes to a deeper understanding of how regional characteristics influence pandemic outcomes. The findings support the need for spatially targeted interventions and underscore the importance of robust spatial analytics in shaping evidence-based public health policies in post-pandemic settings.

Journal of Chemical Health Risks
www.jchr.org
JCHR (2025) 15(5), 306-319 | ISSN:2251-6727

2. Data

This study focuses on 46 Asian countries, excluding regions such as North Korea and Turkmenistan and Russia due to the lack of reliable COVID-19 data. The dataset includes cumulative COVID-19 confirmed cases and deaths per million population (CCCPM, CCDPM) for each country, standardized up to December 2024, to facilitate meaningful spatial comparisons across diverse national contexts. This standardized metric enables a consistent evaluation of disease burden and spatial variation within the Asian region. To ensure spatial precision, country-level administrative boundary shapefiles were obtained from the World Bank's Spatial Boundaries Dataset and integrated using ArcGIS Desktop 10.7 for geospatial analysis and full analysis is done in R-software. The spatial units of analysis correspond to sovereign countries within the Asian continent.

Guided by existing literature on COVID-19 determinants, this study incorporates 17 independent variables (W1-W17) to analyze the spatial heterogeneity of COVID-19 outcomes across Asian countries. These variables reflect key aspects of demographic structure, healthcare infrastructure, socioeconomic status, and environmental exposures relevant to pandemic dynamics. The selection was based on both theoretical justification and empirical evidence.

Variables W1 to W5 represent the prevalence of major pre-existing health conditions such as cancer (W1), cardiovascular diseases (W2), hypertension (W3), diabetes (W4), and respiratory infection-related death rates (W5), which are known to increase vulnerability to severe COVID-19 outcomes. Demographic indicators, including the proportion of the population aged 65 and above (W6), population density (W7), urban population proportion (W8), and life expectancy (W9), help capture population-level risk factors that influence both transmission and mortality rates. Socioeconomic and lifestyle-related factors are included through W10 (current tobacco use), W11 (access to improved sanitation), and W12 (access to improved water sources), which reflect both behavioral risk and basic health service availability. Environmental exposures are captured via W13 (PM 2.5 concentrations) and W14 (death rate due to air pollution), given their role in exacerbating respiratory illnesses and potentially worsening COVID-19 severity.

Lastly, healthcare system capacity and development level are reflected in W15 (hospital beds per thousand people), W16 (current health expenditure as a percentage of GDP), and W17 (Human Development Index), providing a broader view of each country's readiness and resilience in managing health emergencies.

3. The Models and Estimators

To estimate the linear relationship between a dependent variable and one or more independent variables, the Classical Linear Regression Model (CLRM) is employed. The model is specified as

$$y = X\beta + \varepsilon \tag{1}$$

where y is the $n \times 1$ vector of the observations on the dependent variable, X is an $n \times m$ matrix of independent variables, ε is the $n \times 1$ vector of the random errors, and β is the $m \times 1$ vector of the parameters, which is estimated by minimizing the sum of squared residuals and obtained as

$$\hat{\beta} = (X^T X)^{-1} X^T y \tag{2}$$

The estimator in Equation (2) is known as the ordinary least squares (OLS) estimator. Under a set of classical assumptions- linearity, full rank, exogeneity, homoscedasticity, no autocorrelation, and normally distributed errors-the OLS estimator is the Best Linear Unbiased Estimator, according to the Gauss-Markov theorem.

In practice, however, real-world data often violate the assumptions of homoscedasticity and normality due to the presence of extreme values, measurement errors, or heterogeneity. To address these issues, RWLS method is employed. RWLS enhances the classical framework by minimizing a Huber loss function, which provides resistance to outliers and improves stability under heteroscedasticity. The Huber loss $\rho(u)$ is defined as:

$$\rho(u) = \begin{cases} \frac{1}{2}u^2, & \text{if } |u| \le \delta \\ \delta\left(|u| - \frac{1}{2}\delta\right), & \text{if } |u| > \delta \end{cases} \tag{3}$$

Journal of Chemical Health Risks
www.jchr.org
JCHR (2025) 15(5), 306-319 | ISSN:2251-6727

Here, δ is a tuning constant that controls the transition from quadratic to linear loss, providing a compromise between least squares and absolute deviation estimation.

The RWLS estimator minimizes the weighted sum of Huber losses:

$$\hat{\beta}_{RWLS} = \arg\min_{\beta} \sum_{i=1}^{n} w_i \cdot \rho(y_i - X_i^T \beta) \quad (4)$$

where w_i are the observation-specific weights, typically iteratively updated using the Huber influence function:

$$\psi(u) = \begin{cases} u, & \text{if } |u| \le \delta \\ \delta \cdot \text{sign}(u), & \text{if } |u| > \delta \end{cases} \quad (5)$$

This procedure is implemented via Iteratively Reweighted Least Squares (IRLS), where each observation's influence is scaled based on residual magnitude. The RWLS thus serves as a robust generalization of OLS within the classical regression context and is particularly suited for non-spatial datasets contaminated by outliers or non-constant variance.

However, in the presence of spatial dependence, wherein observations are correlated across geographic units, the independence assumption of the CLRM is violated. This may render the OLS and even RWLS estimators inefficient and their inference unreliable. To address this, spatial econometric models such as SLM and SEM are used.

The SLM incorporates spatial dependence directly in the dependent variable:

$$y = \rho W y + X\beta + \varepsilon \quad (6)$$

where ρ is the spatial autoregressive coefficient, and W is a spatial weights matrix capturing the structure of spatial interactions. This model assumes that the value of the dependent variable in one region is influenced by the values in neighboring regions.

The SEM, by contrast, models spatial dependence in the error term:

$$y = X\beta + u, u = \lambda W u + \varepsilon, \quad (7)$$

where λ measures the spatial autocorrelation in the errors. The SEM is particularly useful when the spatial autocorrelation arises from omitted variables or measurement error that are spatially correlated.

While SLM and SEM capture global spatial patterns via spatial weight matrices, they assume spatial stationarity of parameters and thus fail to accommodate regional heterogeneity. To overcome this limitation, GWR is utilized.

GWR models the local relationship between the response and predictors by fitting a separate regression at each location. The GWR model is defined as:

$$y_i = \beta_{i0} + \sum_{j=1}^{m} X_{ij}\beta_{ij} + \varepsilon_i, i = 1,2,\dots,n \quad (8)$$

where y_i is the dependent variable at location i, β_{i0} is the local intercept, X_{ij} and β_{ij} are the j^{th} covariate and its corresponding local coefficient at location i, and ε_i is the error term.

The local coefficients are estimated using:

$$\hat{\beta}(i) = (X^T W(i) X)^{-1} X^T W(i) y \quad (9)$$

where $W(i)$ is a spatial weighting matrix defined by a Gaussian kernel function:

$$W_k(i) = \begin{cases} \exp\left(-\left(\frac{d_{ik}}{bw}\right)^2\right), & \text{if } k \in N_i \\ 0, & \text{otherwise} \end{cases} \quad (10)$$

Here, d_{ik} is the Euclidean distance between locations i and k, bw is the bandwidth, and N_i is the set of nearest neighbors for location i. The kernel assigns higher weights to nearby observations. The bandwidth is chosen via cross-validation (CV), which minimizes:

$$CV(bw) = \sum_{i=1}^{n} \left[y_i - \hat{y}_{(-i)}(bw)\right]^2 \quad (11)$$

Where $\hat{y}_{(-i)}(bw)$ is the predicted value excluding observation i.

Despite its strengths, GWR is sensitive to outliers and heteroscedasticity. To address this limitation, we adopt the RGWR model using Huber weighting, which enhances stability by down-weighting extreme residuals in the local fitting process. The RGWR model retains the same form as Equation (8) but replaces the least squares criterion with a robust objective function based on Huber's loss given in Equation (3).

Journal of Chemical Health Risks
www.jchr.org
JCHR (2025) 15(5), 306-319 | ISSN:2251-6727

Parameter estimation is performed via IRLS, where each observation is assigned a composite weight. This robustified approach improves the estimation of local coefficients in the presence of non-Gaussian errors, heteroscedasticity, or outliers, thereby making spatial modeling more resilient and reliable.

In the following section, we apply the various methodological frameworks discussed above to COVID-19 data across Asian countries. This empirical analysis demonstrates how progressively advanced models enhance the detection and interpretation of spatial patterns, thereby providing deeper insights into the geographic dynamics of the pandemic.

4. Empirical Findings

This section presents the results of the predictive modeling approaches applied to the analysis of COVID-19 outcomes in Asian countries. Building upon the initial observations discussed in the introduction, several diagnostic checks were conducted prior to model estimation to ensure the validity of underlying assumptions.

The exploratory data analysis and spatial visualization of the Asian dataset revealed that the dependent variables (CCCPM, CCDPM) exhibited non-normal distributions, included extreme values (see Figure 1).

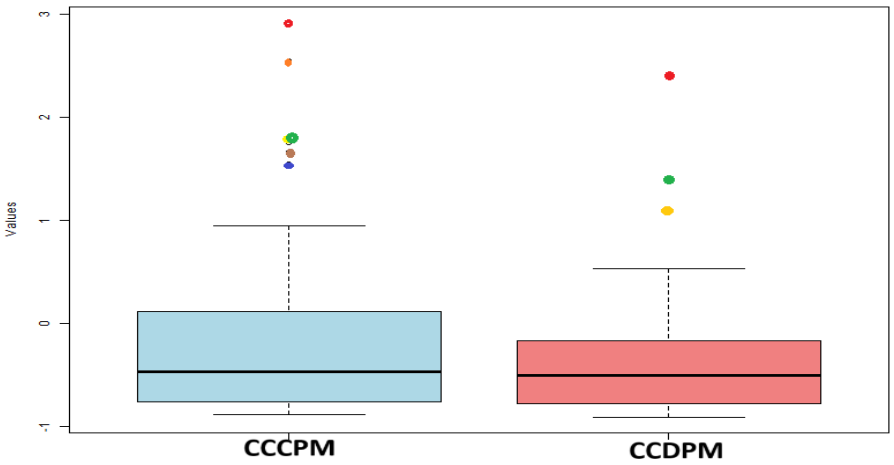

Figure 1. Box-plot Visualization for the Dependent Variables.

Furthermore, spatial dependence was confirmed by the Global Moran's I values of 0.71 for CCCPM (p-value = 0.0001) and 0.68 for CCDPM (p-value = 0.0002), both of which are highly significant, indicating strong positive spatial clustering in the data.

Based on the diagnostic results discussed earlier, the data for Asian countries exhibited key issues such as non-normal distribution, the presence of outliers, and spatial dependence in the dependent variables. To address these issues, the RWLS model was first employed to reduce the influence of non- normality and outliers. However, due to the significant spatial dependence detected among observations, spatial regression models—including SLM, SEM, GWR, and RGWR—were subsequently applied. Each model was introduced to incrementally overcome the limitations of the preceding one, enabling a more refined understanding of spatial and structural variations in COVID-19 outcomes across Asia. The findings and comparative performance of these models are discussed in the following subsections. To evaluate model performance in the Asian context, the dataset was partitioned into training (80%) and testing (20%) subsets. The training set was used to estimate model parameters, while the test set was reserved for evaluating predictive accuracy on unseen data.

4.1 Comparison of Predicted and Actual Values

This section presents a comparative analysis between the actual and predicted values generated by the

Journal of Chemical Health Risks
www.jchr.org
JCHR (2025) 15(5), 306-319 | ISSN:2251-6727

models: RWLS, SLM, SEM, GWR and RGWR. The primary objective is to assess how accurately each model captures the spatial distribution and underlying trends present in the data. To assess both model fit and generalization, a 20% hold-out sample was used for evaluating predictive accuracy. Figure 2 then compare actual and predicted CCCPM and CCDPM values, offering a visual insight into each model's performance across the region.

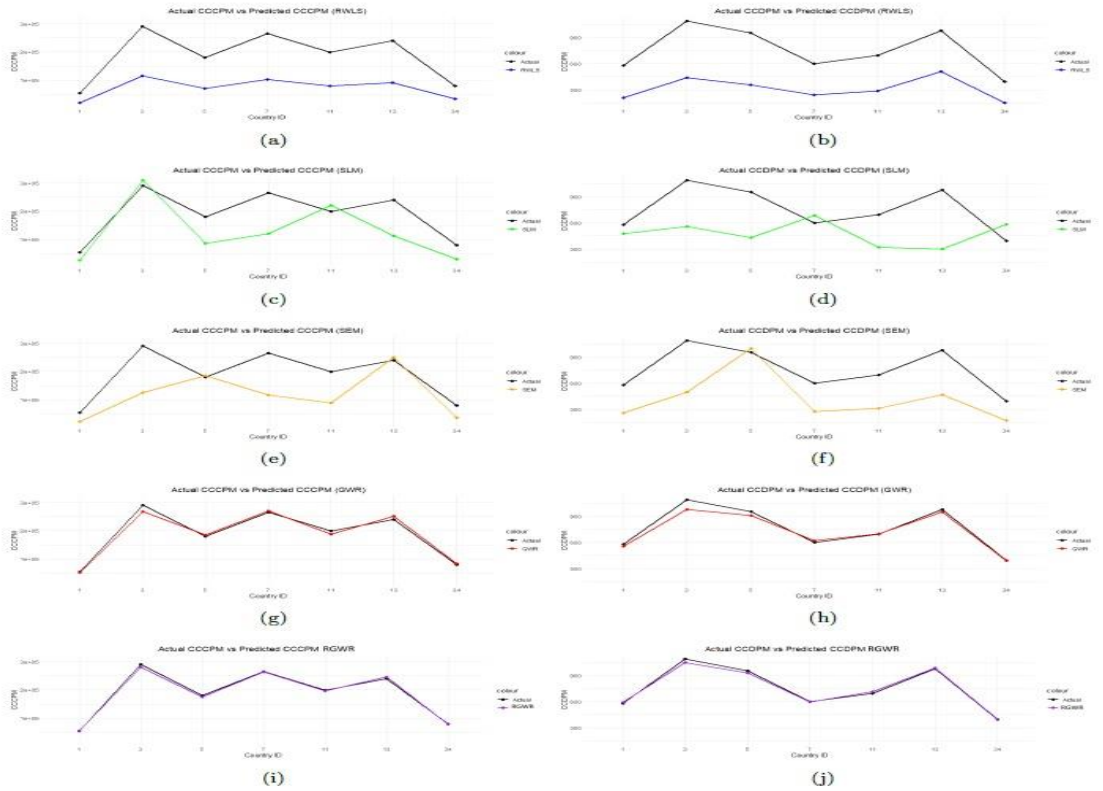

Figure 2. Visual comparison of actual vs. predicted CCCPM (left) and CCDPM (right) across all predictive models.

As illustrated in Figure 2, the comparison between predicted and actual values reveals distinct differences in model performance. The graphical analysis highlights the superior performance of the GWR and RGWR models in predicting both CCCPM and CCDPM. While the GWR model's predictions closely follow the actual values, the RGWR model provides even better alignment, indicating its enhanced ability to capture underlying spatial patterns and regional variability in the data. In contrast, the RWLS, SLM, and SEM models show notable deviations from actual values. Although RWLS handles outliers well, it tends to underestimate outcomes. SLM and SEM account for spatial dependence but apply it uniformly, missing local variations—leading to less accurate predictions in many regions. These observed differences seen in Figure 2 in predictive alignment will be further examined using statistical evaluation metrics: Adj. R^2, RMSE, AIC, and BIC. Adj. R^2 reflects explanatory power while adjusting for model complexity; higher values indicate better fit. RMSE measures prediction accuracy, with lower values signifying greater precision. AIC and BIC evaluate model fit with penalties for complexity, where lower values suggest more efficient models. These metrics offer a comprehensive comparison of how well each model captures spatial patterns and predicts COVID-19 outcomes. The summary of results is presented in Table 1, highlighting differences in model performance.

Journal of Chemical Health Risks
www.jchr.org
JCHR (2025) 15(5), 306-319 | ISSN:2251-6727

Table 1. Comparison of Performance Metrics Across Predictive Models for CCCPM and CCDPM in Asia

CCCPM	CCDPM	
Models	Adj. R_2 RMSE AIC BIC	Adj. R_2 RMSE AIC BIC
RWLS	0.383 0.638 127.450 161.230	0.331 0.329 466.750 451.260
SLM	0.425 0.494 104.980 117.930	0.417 0.393 351.780 422.310
SEM	0.437 0.521 112.690 110.540	0.424 0.409 359.210 412.870
GWR	0.881 0.336 77.890 58.410	0.913 0.348 302.740 372.110
RGWR	0.9179 0.316 77.190 57.937	0.926 0.334 295.980 367.540

As shown in Table 1, the RGWR model outperforms all others, achieving the highest Adj. R^2 for CCCPM (0.918) and CCDPM (0.926), along with the lowest RMSE, AIC, and BIC values. This indicates strong explanatory power, high predictive accuracy, and efficient model complexity. RGWR's ability to handle spatial non-stationarity, heteroscedasticity, and outliers makes it particularly effective in capturing localized spatial heterogeneity in COVID-19 outcomes. Given its superior performance, the next subsection evaluates RGWR's residuals to assess key assumptions, including homoscedasticity and spatial independence, ensuring the model's robustness for interpretation.

4.2 Residual Diagnostics of RGWR Model

In this section, we assess the robustness and stability of the RGWR model through residual diagnostics, using the GWR model as a baseline for comparison, given its established role as a standard method for capturing spatial non-stationarity. This included examining the distribution of residuals through boxplots and evaluating the presence of heteroscedasticity using the Breusch- Pagan (BP) test. To evaluate the influence of outliers, we examined the residual distributions of the GWR and RGWR models through boxplot visualization, as shown in Figure 3.

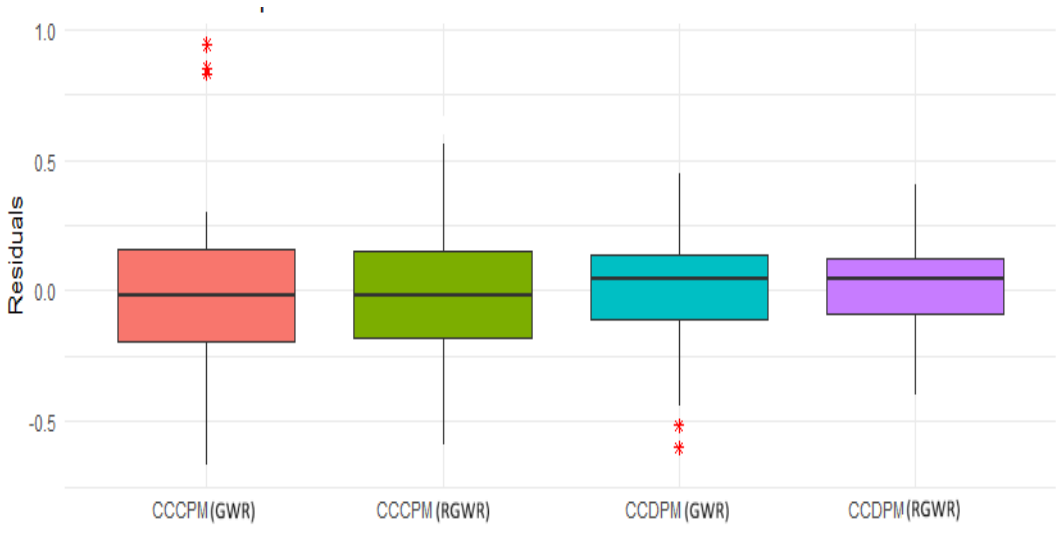

Figure 3. Boxplot of GWR and RGWR Residuals

Journal of Chemical Health Risks
www.jchr.org
JCHR (2025) 15(5), 306-319 | ISSN:2251-6727

According to the figure, the GWR model exhibits heavy-tailed residuals with several extreme values, indicating a pronounced sensitivity to outliers and the presence of heteroscedasticity. In contrast, the RGWR model produces a more symmetric and compact residual distribution, reflecting a reduced influence of extreme observations and improved robustness. This suggests that the RGWR model demonstrates greater residual stability and consistency.

This enhanced robustness is further supported by the Breusch–Pagan (BP) test results. For the RGWR model, the BP test statistics were 3.82 for CCCPM and 4.74 for CCDPM, with corresponding p-values greater than 0.05. These results confirm the homoscedastic nature of the residuals in the RGWR model, strengthening the evidence for its superior fit and reliability.

RGWR demonstrates the best overall performance, with the highest adjusted R^2, lowest RMSE, and favourable AIC and BIC values—indicating strong explanatory power and robustness to spatial heterogeneity and outliers. While GWR accounts for spatial variation better than OLS, SLM, and SEM, it remains sensitive to data irregularities. RGWR overcomes these limitations, offering a more resilient framework for modeling COVID-19 spread. Given its superior performance across all metrics, key results from the RGWR model are discussed in the following subsections.

4.3 Key Findings from RGWR model

The optimal bandwidths selected by the RGWR model are slightly higher than those of the GWR model (CCCPM: 0.346 vs. 0.312; CCDPM: 0.307 vs. 0.291), indicating that RGWR draws information from a broader spatial neighborhood. This broader bandwidth enhances local adaptation while maintaining robustness. Furthermore, RGWR incorporates a tuning parameter (0.034 for CCCPM; 0.057 for CCDPM), which improves model stability and accuracy by reducing sensitivity to outliers and heteroscedasticity.

Similar to the GWR model, RGWR generates spatially varying coefficient estimates, meaning the effect of each explanatory variable differs across locations. This localized modeling approach enables RGWR to better capture spatial non-stationarity by assigning unique coefficient values to each spatial unit, rather than assuming a constant effect across the entire study area. As demonstrated in the previous section, the RGWR model outperformed all other models. This section discussed the coefficient estimates obtained from the RGWR model applied to the CCCPM and CCDPM data across Asian countries.

The subsection is organized into two subsubsections: the first discusses key findings related to CCCPM, and the second focuses on CCDPM.

Key Findings from the RGWR Model for CCCPM

The coefficient estimates of RGWR model results for CCCPM across Asian countries given in Table 2, reveal a diverse range of influences from different groups of variables, including health-related, demographic, socioeconomic, and environmental factors.

Table 2. Summary Statistics of RGWR Model Coefficients for CCCPM in Asian countries

Variable	Min.	Q1	Median	Mean	Q3	Max.
Intercept	-0.4967	0.0864	0.2914	0.2376	0.4425	0.5560
W1	-0.9358	-0.5018	0.1639	0.2260	0.0951	0.2775
W2	-0.6087	-0.4008	0.2089	0.2618	-0.0920	-0.0318
W3	-0.0909	0.0159	0.0825	0.0780	0.1363	0.2253
W4	-0.2187	-0.1209	0.0903	0.0634	0.0230	0.0467
W5	-1.1951	-0.5095	-0.2261	-0.3247	-0.0547	0.0081
W6	-0.9536	-0.5372	0.3656	0.3234	1.2570	1.6141
W7	0.1674	0.2980	0.4099	0.6723	1.0891	1.3736

Journal of Chemical Health Risks
www.jchr.org
JCHR (2025) 15(5), 306-319 | ISSN:2251-6727

W8	-0.1013	0.1107	0.4137	0.3288	0.5072	0.6339
W9	-0.7337	-0.2992	-0.0370	0.0736	0.5101	1.3148
W10	-0.1052	-0.0208	0.0243	0.0204	0.0659	0.1469
W11	-1.0264	-0.6545	0.0424	0.1865	0.1723	0.3469
W12	-0.2082	-0.0851	0.5044	0.4747	1.0186	1.3028
W13	-0.1245	0.0711	0.1355	0.1540	0.2734	0.4045
W14	-0.7900	-0.6006	-0.5161	-0.3686	-0.2556	1.0239
W15	-0.4913	-0.4064	-0.1470	-0.0682	0.2653	0.4856
W16	-0.5034	-0.3147	0.0478	-0.0506	0.1472	0.2641
W17	0.0119	0.0759	0.1934	0.1980	0.3235	0.3898

As referenced to the Table 2, The RGWR model results reveal that several variables significantly influence CCCPM across Asian countries, though their effects vary spatially. Among health-related factors, the prevalence of cancer (W1) and cardiovascular disease (W2) show strong and consistently positive mean coefficients (0.226 and 0.262, respectively), indicating their significant role in increasing COVID-19 case rates—likely due to compromised immunity and overlapping risk profiles. Hypertension (W3) and diabetes (W4) also exhibit positive effects, albeit to a slightly lesser degree, further supporting their contribution to vulnerability. Conversely, deaths from respiratory infections (W5) display a significant negative mean effect (-0.325), suggesting potential underreporting or diagnostic overlap in countries with a high respiratory disease burden.

Among demographic variables, the proportion of the elderly population (W6) and population density (W7) stand out with strong positive effects (mean: 0.323 and 0.672, respectively), confirming that older populations and denser regions face greater exposure and risk. Similarly, the urban population share (W8) and life expectancy (W9) exhibit positive influences, although with more variability.

From the socioeconomic dimension, the Human Development Index (W17) shows a consistent and significant positive effect (mean: 0.198), suggesting that more developed countries tend to detect and report more cases due to stronger healthcare and surveillance systems. Likewise, access to improved water sources (W12) and sanitation (W11) display positive mean effects (0.475 and 0.187), likely reflecting the role of better infrastructure in supporting case detection, although sanitation's influence is relatively moderate.

Among environmental and infrastructure variables, PM2.5 pollution (W13) has a significant positive impact (mean: 0.154), underscoring the role of air quality in respiratory vulnerability and viral transmission. In contrast, death from air pollution (W14) and hospital beds per 1,000 population (W15) show mixed and weaker effects. While health expenditure as a percentage of GDP (W16) shows some positive influence in the upper range, its overall impact remains relatively small.

In summary, the most significant predictors of COVID-19 case rates in Asia include cancer and cardiovascular prevalence, population density, elderly population share, PM 2.5 pollution, improved water access and sanitation facilities, and HDI. Other variables demonstrate weaker or more inconsistent effects, emphasizing the spatial heterogeneity in pandemic dynamics across the region.

The observed variability in coefficients across variables highlights spatial heterogeneity in the data, emphasizing that the influence of predictors varies across different countries. The spread between minimum and maximum values captures this regional variation, while median values reflect central tendencies. These findings underscore the utility of spatially adaptive models like RGWR to capture such differences and provide more accurate information on the determinants of the spread of COVID-19 globally.

As discussed earlier, each selected independent variable influences different geographic units in distinct ways. This results in a varying range of significant variables explaining the variance in CCCPM across

Journal of Chemical Health Risks
www.jchr.org
JCHR (2025) 15(5), 306-319 | ISSN:2251-6727

countries. On average, the RGWR model accounts for 91% of the variation in CCCPM, though the explanatory power varies across regions. The Figure 4 displays the local adj. R^2 values, which indicate the proportion of variance explained by the selected variables in each spatial unit. As shown in Figure 4, the local adj R^2 values derived from the RGWR model for CCCPM across Asian countries range from 0.879 to 0.939, with a mean of 0.918 and a median of 0.915. These consistently high values indicate that the selected explanatory variables collectively account for more than 87% of the variation in COVID-19 deaths per million at the local level across the region.

For at least three-fourths of the countries, the local adj R^2 values lie above 0.90, demonstrating very strong explanatory power of the model in most locations. The lowest quartile (Q1 = 0.905) still reflects robust fit, with even the minimum value (0.879) indicating a reasonably good level of model performance. This pattern suggests relatively low spatial heterogeneity in model performance across Asia, with only minor variation in explanatory strength across countries.

Specifically, countries such as India, China, Indonesia, Pakistan, Japan, South Korea, Bangladesh, Vietnam, and the Philippines, along with other nations like Saudi Arabia, Iran, Turkey, and the UAE, show strong local adj R^2 values, indicating that the selected health, demographic, socioeconomic, and environmental predictors are highly effective in explaining COVID-19 death rates across these diverse national contexts. Thus, the consistently high local adj R^2 across the 46 Asian countries listed confirms the strong spatial performance and robustness of the RGWR model in capturing region-specific influences on CCCPM.

Similarly, the key findings from the RGWR model for CCDPM across world are presented in the following subsubsection.

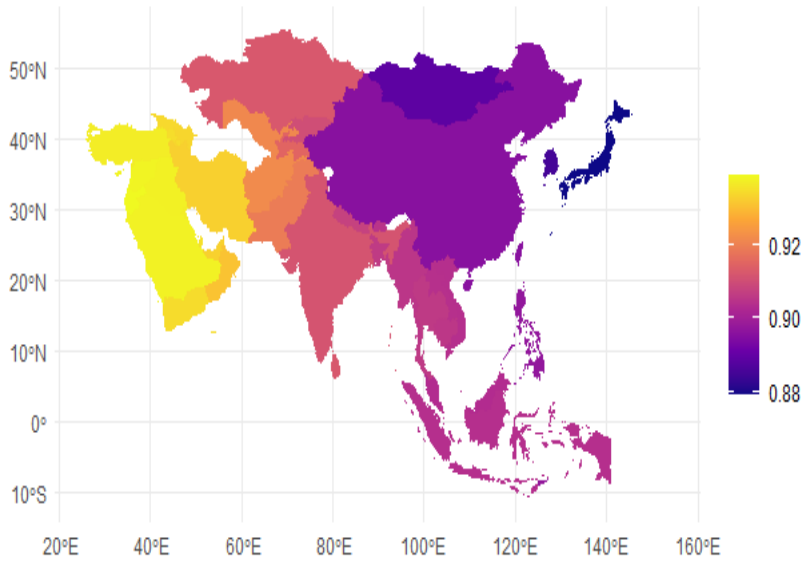

Figure 4. Choropleth maps for the distribution of local adj. R^2 for RGWR model, CCCPM.

Key Findings from the RGWR Model for CCDPM

The coefficient estimates of the RGWR model results for CCDPM across Asian countries, as presented in Table 3, reveal a diverse range of influences from various groups of variables, including health-related, demographic, socioeconomic, and environmental factors The RGWR model results for CCDPM across Asian countries highlight several variables with significant and consistent impacts on COVID-19 mortality. Among health-related variables, the prevalence of cardiovascular disease (W2) stands out as a strong predictor, with a high mean coefficient of

Journal of Chemical Health Risks
www.jchr.org
JCHR (2025) 15(5), 306-319 | ISSN:2251-6727

0.298 and a maximum of 0.569, indicating that regions with higher cardiovascular burden experience greater mortality. Hypertension (W3) also shows a consistently positive and significant effect (mean: 0.184), reinforcing its role as a comorbidity linked to severe outcomes. Interestingly, diabetes prevalence (W4), though showing a slightly negative lower bound, presents a positive mean (0.171) and median, suggesting it is also an important mortality risk factor in many regions.

Demographic characteristics, especially the proportion of elderly population (W6), exert a strong and consistent influence, with a mean coefficient of 0.705 and a maximum of 1.286, making it one of the most significant contributors to COVID-19 deaths. experience elevated death rates, though its impact is less pronounced than other variables.

Table 3. Summary Statistics of RGWR Model Coefficients for CCDPM in Asian Countries

Variable	Min	Q1	Median	Mean	Q3	Max
Intercept	-0.43490	-0.30186	-0.26239	-0.24603	-0.18468	-0.02836
W1	-0.22550	-0.12214	-0.08309	-0.03264	0.07397	0.26894
W2	0.18900	0.21370	0.25900	0.29780	0.39350	0.56910
W3	0.07749	0.12172	0.18477	0.18426	0.14458	0.25191
W4	-0.13981	-0.10925	0.17639	0.17066	0.03170	0.21071
W5	-1.62983	-1.01016	-0.15818	-0.41986	0.07281	0.16827
W6	0.15980	0.35190	0.81480	0.70510	1.05820	1.28610
W7	-0.18910	-0.14445	-0.05532	0.10485	0.39864	0.66396
W8	-0.16305	-0.06335	-0.02465	-0.02786	0.01383	0.07668
W9	-0.18943	-0.10551	0.00053	-0.02760	0.02369	0.17647
W10	-0.03862	0.04643	0.13234	0.10499	0.15642	0.19409
W11	0.03027	0.10496	0.19545	0.34708	0.61969	1.31192
W12	-0.17510	-0.12492	-0.03727	0.07432	0.30957	0.69622
W13	-0.12331	-0.06506	-0.00175	-0.02916	0.00966	0.02764
W14	-0.56434	-0.15296	-0.11325	-0.05513	0.07784	0.21103
W15	-0.33151	-0.22579	-0.17455	-0.18664	-0.15103	0.02252
W16	0.06809	0.12106	0.15112	0.14770	0.17494	0.24789
W17	0.20020	0.32070	0.35300	0.38650	0.48400	0.60850

Population density (W7) shows a moderate positive effect overall (mean: 0.105). Among socioeconomic factors, improved sanitation (W11) emerges as a notable predictor, with a mean of 0.347 and a maximum of 1.312, possibly reflecting the association between better infrastructure and improved reporting of deaths or exposure levels in urbanized environments. Health expenditure (W16) and the Human Development Index (W17) also demonstrate consistently positive effects, with mean values of 0.148 and 0.387, respectively, suggesting that countries with better healthcare investment and development levels are more likely to report COVID-19 deaths accurately.

Tobacco use (W10) shows a moderately positive influence (mean: 0.105), aligning with its known association with respiratory vulnerability. Other variables, such as air pollution (W13) and hospital beds (W15), show weaker or even negative mean effects, indicating more complex or location-dependent relationships. The death rate from respiratory infections (W5) shows a negative mean (-0.420) but wide variability, suggesting that in areas with high baseline respiratory mortality, COVID-19 deaths may be underreported or misclassified.

In summary, the most significant variables influencing COVID-19 deaths per million in Asia are W2 (cardiovascular disease), W3 (hypertension), W4 (diabetes), W6 (elderly population), W11 (sanitation), W16 (health expenditure), and W17 (HDI). These findings highlight the critical role of underlying health conditions, age structure, and healthcare capacity in shaping mortality patterns

Journal of Chemical Health Risks
www.jchr.org
JCHR (2025) 15(5), 306-319 | ISSN:2251-6727

during the pandemic across Asian regions. Other variables demonstrate weaker or more inconsistent effects, emphasizing the spatial heterogeneity of pandemic impacts.

As discussed earlier, the RGWR model accounts for significant spatial variation in CCDPM across regions. The range of coefficients and the local adjusted R^2 values (Figure 5) further illustrate how different factors explain the variance in CCDPM, with explanatory power varying by region.

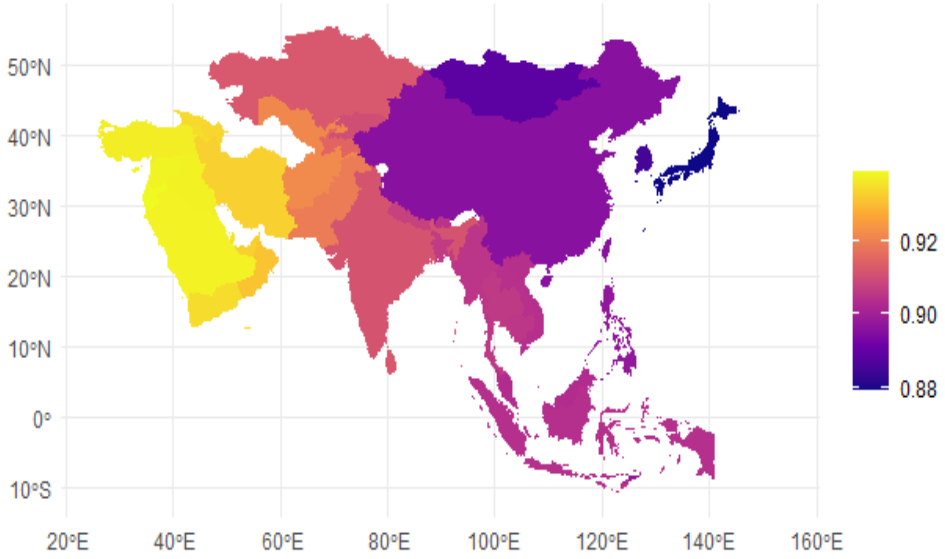

Figure 5. Choropleth maps for the distribution of local adj. R^2 for RGWR model, CCDPM

As shown in Figure 5, the local adj R^2 values derived from the RGWR model for CCDPM across Asian countries range from 0.879 to 0.949, with a mean of 0.928 and a median of 0.925. These consistently high values indicate that the selected explanatory variables collectively account for more than 87% of the variation in COVID-19 deaths per million at the local level across the region.

For at least three-fourths of the countries, the local adj R^2 values lie above 0.915, demonstrating very strong explanatory power of the model in most locations. The lowest quartile (Q1 = 0.915) still reflects a robust fit, with even the minimum value (0.879) indicating a reasonably good level of model performance. This pattern suggests relatively low spatial heterogeneity in model performance across Asia, with only minor variation in explanatory strength across countries. Specifically, countries such as India, China, Indonesia, Pakistan, Japan, South Korea, Bangladesh, Vietnam, and the Philippines, along with other nations like Saudi Arabia, Iran, Turkey, and the UAE, show strong local adj R^2 values, indicating that the selected health, demographic, socioeconomic, and environmental predictors are highly effective in explaining COVID-19 death rates across these diverse national contexts.

Thus, the consistently high local adj R^2 across the entire set of 46 Asian countries listed confirms the strong spatial performance and robustness of the RGWR model in capturing region-specific influences on CCDPM.

These findings confirm the value of the RGWR model in capturing the spatial dynamics of COVID-19 mortality, highlighting the importance of location-specific factors in explaining CCDPM. The observed variability in explanatory power and predictor significance across countries reinforces the need for targeted public health strategies.

The following section presents a summary of the key findings from this chapter, highlighting the main results and their implications for understanding global patterns in COVID-19 outcomes.

Journal of Chemical Health Risks

www.jchr.org

JCHR (2025) 15(5), 306-319 | ISSN:2251-6727

5. Summary

This chapter examined a range of modeling approaches to understand and predict the spread of COVID-19 across Asian countries. The analysis began by exploring key patterns through exploratory data analysis and spatial visualization. These analyses revealed important issues, such as the non-normal distribution of the dependent variables, the presence of extreme outliers, and significant spatial clustering of CCCPM and CCDPM within the region. These observed patterns underscored the necessity of employing both robust and spatial modeling strategies to accurately capture the complex dynamics of the pandemic in the Asian context.

To address the challenges of non-normality and outliers, we first employed the RWLS model as part of the classical regression approach. This model provided more stable coefficient estimates by reducing the influence of outliers and accounting for heteroscedasticity. However, spatial visualization indicated significant spatial dependence, prompting the use of spatial regression models, specifically, the SLM, SEM, and GWR. Among these, GWR was particularly effective in capturing spatial non-stationarity in the relationships between predictors and COVID-19 outcomes.

Despite the strengths of GWR, residual diagnostics indicated its sensitivity to outliers and heteroscedasticity. To address these limitations, the RGWR model was introduced. This enhanced approach integrates the Huber weights framework for robustness and employs adaptive bandwidth selection to improve spatial fit. The RGWR model preserved the spatial adaptability of GWR while offering improved predictive performance, as evidenced by reductions in RMSE, AIC, and BIC, along with higher adjusted R^2 values. On average, the RGWR model accounted for approximately 91% of the variation in CCCPM and 92% in CCDPM, reflecting its superior modeling capability.

Importantly, RGWR provides country-specific coefficient estimates, revealing that different regions are influenced by distinct risk factors. This spatial heterogeneity underscores the need for localized public health strategies.

This study highlights that certain variables—such as the proportion of elderly population, air pollution indicators, and health system factors like hospital beds and health expenditure—consistently emerged as significant across all models for both CCCPM and CCDPM. Variables like cardiovascular disease prevalence and the Human Development Index also appeared frequently, underscoring their broad relevance. Notably, as more advanced and spatially adaptive models were employed (e.g., GWR and RGWR), the selection of significant variables became more nuanced and aligned with contextual factors, thereby enhancing the interpretability and policy relevance of the findings.

These findings emphasize the importance of using advanced predictive models like RGWR, which integrate spatial adaptability and robustness. Such models provide a more accurate and nuanced understanding of pandemic dynamics and can play a crucial role in informing targeted, region- specific public health interventions and resource allocation in future health emergencies.

References

1. Adekunle, I. A., Onanuga, A. T., Akinola, O. O., & Ogunbanjo, O. W. (2020). Modelling spatial variations of coronavirus disease (COVID-19) in Africa. *Science of the Total Environment, 729,* 138998.
2. Ahmed, F., Ahmed, N., Pissarides, C., & Stiglitz, J. (2020). Why inequality could spread COVID-19. *The Lancet Public Health, 5*(5), e240.
3. Anselin, L. (1988). *Spatial Econometrics: Methods and Models.* Dordrecht: Springer.
4. Appiah-Otoo, I., & Kursah, M. B. (2022). Modelling spatial variations of novel coronavirus disease (COVID-19): Evidence from a global perspective. *GeoJournal, 87*(4), 3203–3217.
5. Bashir, M. F., Ma, B., Komal, B., Bashir, M. A., Tan, D., Bashir, M., *et al.* (2020). Correlation between climate indicators and COVID-19 pandemic in New York, USA. *Science of the Total Environment, 728,* 138835.
6. Chandra, S., & Sharma, M. (2024). Determinants of COVID-19 prevalence rate in Asia: A study using spatial analysis. *Indian Journal of Public Health Research & Development, 15*(2), 333–341.

Journal of Chemical Health Risks

www.jchr.org

JCHR (2025) 15(5), 306-319 | ISSN:2251-6727

7. Chaurasia, R., Singh, S., & Singh, V. (2021). Progression of COVID-19 in India: A linear regression analysis. *medRxiv.*
8. Chen, B., Liang, H., Yuan, X., Hu, Y., Xu, M., Zhao, Y., Zhang, B., Tian, F., & Zhu, X. (2020). Roles of meteorological conditions in COVID-19 transmission on a worldwide scale. *BMJ Open, 10*(e041397).
9. Chen, Y., Okada, N., & Zhou, Y. (2012). Geographically weighted regression based on the asymmetric loss function. *Stochastic Environmental Research and Risk Assessment, 26*(6), 799–810.
10. Chi, G., Zhu, J., & et al. (2021). Spatial regression models for COVID-19 incidence and mortality in the United States. *International Journal of Environmental Research and Public Health, 18*(3), 1042.
11. Chung, H. W., Apio, C., Goo, T., Heo, G., Han, K., Kim, T., Kim, H., Ko, Y., Lee, D., Lim, J., *et al.* (2021). Effects of government policies on the spread of COVID-19 worldwide. *Scientific Reports, 11*(1), 20495.
12. Desjardins, M. R., Hohl, A., & Delmelle, E. M. (2020). Space-time COVID-19 monitoring using smart detection and spatial modeling: A case study in the US. *International Journal of Health Geographics, 19*(1), 1–16.
13. Dutta, I., Basu, T., & Das, A. (2021). Spatial analysis of COVID-19 incidence and its determinants using spatial modeling: A study on India. *Environmental Challenges, 4,* 100096.
14. Elhorst, J. P. (2014). *Spatial econometrics: From cross-sectional data to spatial panels.* Springer Briefs in Regional Science. Springer.
15. Fotheringham, A. S., Brunsdon, C., & Charlton, M. (2002). *Geographically weighted regression: The analysis of spatially varying relationships.* Wiley.
16. Kumar, A., & Awasthi, A. (2020). Piecewise linear regression for predicting COVID-19 cases in India. *Modeling and Simulation in Engineering,* 2020, 1–7.
17. LeSage, J. P. (2004). A family of geographically weighted regression models. In L. Anselin, R. Florax, & S. J. Rey (Eds.), *Advances in spatial econometrics* (pp. 241–264). Springer.
18. Pereira, M., & Oliveira, A. M. (2020). Poverty and food insecurity may increase as the threat of COVID-19 spreads. *Public Health Nutrition, 23*(17), 3236–3240.
19. Ramírez-Aldana, R., Gomez-Verjan, J. C., & Bello-Chavolla, O. Y. (2020). Spatial analysis of COVID-19 spread in Iran: Insights into geographical and structural transmission determinants at a province level. *PLoS Neglected Tropical Diseases, 14*(11), e0008875.
20. Rocklöv, J., & Sjödin, H. (2020). High population densities catalyse the spread of COVID-19. *Journal of Travel Medicine, 27*(3), taaa038.
21. Sardar, S., Abdul-Khaliq, I., Ingar, A., Amaidia, H., & Mansour, N. (2020). COVID-19 lockdown: A protective measure or exacerbator of health inequalities? A comparison between the United Kingdom and India. *International Journal of Surgery, 83,* 189–191.
22. Sarkar, S. K., Ekram, K. M. M., & Das, P. C. (2021). Spatial modeling of COVID-19 transmission in Bangladesh. *Spatial Information Research,* 29, 731–742.
23. Sharma, M., & Chandra, S. (2024). Exploring COVID-19 spatial patterns in Indian districts: Ridge and Lasso geographically weighted models for spatial heterogeneity and multicollinearity. *Founded 1998,* 143.
24. Sridhar, K. S. (2023). Urbanization and COVID-19 prevalence in India. *Regional Science Policy & Practice, 15*(3), 493–505.
25. Tosepu, R., Gunawan, J., Effendy, D. S., Lestari, H., Bahar, H., & Asfian, P., et al. (2020). Correlation between weather and COVID-19 pandemic in Jakarta, Indonesia. *Science of the Total Environment, 725,* 138436.
26. Zhang, J., & Mei, C. L. (2011). Local least absolute deviation estimation of spatially varying coefficients models: Robust geographically weighted regression approaches. *International Journal of Geographical Information Science, 25*(9), 1417–1438.